Accident Analysis and Prevention 206 (2024) 107695

Contents lists available at ScienceDirect

Accident Analysis and Prevention

journal homepage: www.elsevier.com/locate/aap

Analyzing speed-difference impact on freeway joint injury severities of Leading-Following vehicles using statistical and data-driven models

Chenzhu Wang [a], Mohamed Abdel-Aty [a], Lei Han [a,*], Said M. Easa [b]

[a] Department of Civil, Environmental & Construction Engineering, University of Central Florida, Orlando, FL 32816, United States
[b] Department of Civil Engineering, Toronto Metropolitan University, Toronto, Ontario, M5B 2K3, Canada

ARTICLE INFO

Keywords:
Rear-end (RE) crashes
Injury severity
Speed difference
Cross-stitch multilayer perceptron network

ABSTRACT

Rear-end (RE) crashes are notably prevalent and pose a substantial risk on freeways. This paper explores the correlation between speed difference among the following and leading vehicles (Δv) and RE crash risk. Three joint models, comprising both uncorrelated and correlated joint random-parameters bivariate probit (RPBP) approaches (statistical methods) and a cross-stitch multilayer perceptron (CS-MLP) network (a data-driven method), were estimated and compared against three separate models: Support Vector Machines (SVM), eXtreme Gradient Boosting (XGBoost), and MLP networks (all data-driven methods). Data on 15,980 two-vehicle RE crashes were collected over a two-year period, from January 1, 2021, to December 31, 2022, considering two possible levels of injury severity: no injury and injury/fatality for both drivers of following and leading vehicles. The comparative performance analysis demonstrates the superior predictive capability of the CS-MLP network over the uncorrelated/correlated joint RPBP model, SVM, XGBoost, and MLP networks in terms of recall, F-1 Score, and AUC. Significantly, numerous shared variables influence the injury severity outcomes for the following and leading vehicles across both statistical and data-driven approaches. Among these factors, the following vehicle (a truck) and the leading vehicle (a passenger car) demonstrate contrasting effects on the injury severity outcomes for both vehicles. Furthermore, the SHapley Additive exPlanations (SHAP) values from the CS-MLP network visually show the relationship between Δv and injury severity, revealing non-linear trends unlike the average effects shown by statistical methods. They indicate that the least injury outcomes for both following and leading vehicles occurs at a Δv of 0 to 10 mph, matching observed patterns in RE crash data. Additionally, a marked variation in the trend of SHAP values for the two vehicles is noted as the speed difference increases. Therefore, the findings affirm the superior performance of joint model development and substantiate the non-linear impacts of speed difference on injury outcomes. The adoption of dynamic speed control measures is recommended to mitigate the injury outcomes involved in two-vehicle RE crashes.

1. Introduction

Nowadays, with serious injuries and fatalities on freeways, rear-end (RE) crashes cause critical safety and economic concerns worldwide. In 2020, these crashes represented the most frequent type of crashes in the United States, accounting for 27.8 % of all reported crashes, according to the National Highway Traffic Safety Administration (NHTSA, 2020). Approximately 29 % of all traffic crashes resulting in serious injuries are RE crashes (Richard, 2021). Furthermore, they account for more than 7 % of all traffic-related fatalities, with nearly 20 % of these fatalities involving two-vehicle crashes (Richard, 2021). The injuries sustained in RE crashes can be severe and diverse, including whiplash, back and spinal injuries, traumatic brain injuries, and broken bones (Anderson and Baldock, 2008). Given these facts, it is crucial to conduct an in-depth examination of the risk factors linked to rear-end crashes and devise efficient countermeasures to diminish the risks and negative consequences associated with these crashes.

Recent research has increasingly focused on the injury severities of RE crashes (Chatterjee, 2016; Chen et al., 2016). In such crashes, the involved drivers share the same environmental conditions, including the roadway, weather, and lighting, and may be influenced by each other's driving behaviors and vehicle states and operating speed (Wang et al., 2022a). Consequently, current research has begun to analyze the injury severities of both drivers involved in two-vehicle crashes. For example,

* Corresponding author.
E-mail addresses: chenzhu.wang@ucf.edu (C. Wang), M.aty@ucf.edu (M. Abdel-Aty), le966091@ucf.edu (L. Han), seasa@torontomu.ca (S.M. Easa).

https://doi.org/10.1016/j.aap.2024.107695
Received 9 April 2024; Received in revised form 20 June 2024; Accepted 28 June 2024
Available online 6 July 2024

Rana et al. (2010) simultaneously modeled the injury outcomes of drivers in two-vehicle crashes using a copula-based method. Similarly, Song et al. (2023) developed a random parameter bivariate probit (RPBP) model to examine drivers' injury outcomes in truck-car crashes. Wang et al. (2024a) further explored a correlated RPBP model, including heterogeneity in means, to study the impact of speed difference on injury severity in freeway RE crashes. This sophisticated modeling framework comprehensively captures the interplay among the injury severity outcomes of both drivers and addresses the impact of unobserved heterogeneity.

Speed, as a primary risk factor in traffic safety, escalates both the frequency and the severity of injuries in crashes (Hauer, 2009). Many scholars have devoted their efforts to exploring the association between speed and crash risk (Elvik et al., 2019). Elvik (2013) analyzed the relationship between speed and road safety and indicated that a power function best fits the data for fatal crashes. Soole et al. (2013) found that reductions in crash rates have also been associated with average speed enforcement, particularly in relation to fatal and serious injury crashes. Li et al. (2021) analyzed vehicle trajectory data to evaluate the risk of rear-end crashes, revealing an elevated risk of such crashes with larger speed differentials. Doecke et al. (2021) noted higher risk of being severely injured with greater travel speed. They also revealed variations in the magnitude of increase among different types of crashes, including head-on, RE, and single-vehicle crashes. Given this, using advanced methods to examine the effects of speed differences on drivers' injury severity outcomes in two-vehicle RE crashes could yield novel insights, aid understanding, and inform safety enhancements.

However, the concerns of missing data and variations in unobserved effects like driving behaviors and safety manner, influenced by economic, socio-demographic, and vehicle factors, can increase estimation bias. To address this unobserved heterogeneity (Mannering et al., 2016), numerous data-driven methods have been proposed in safety analysis. These encompass data mining, artificial intelligence, and machine learning, augmenting the extensions of traditional safety models (Mannering, 2018). Recently, a notable increase in research efforts has been dedicated to examining injury severity outcomes using machine learning methods. Santos et al. (2022) compared 25 different machine-learning techniques and found that the Random Forest algorithm yielded the best results. However, considerable scope remains for further exploration in jointly addressing both model performance and causality issues, along with unobserved heterogeneity. While data-driven methods are proficient in handling large datasets and providing high predictive accuracy, they often do not offer substantial insights into the causality underlying traffic crashes. In contrast, advanced statistical methods, especially those that address endogeneity and heterogeneity, are better suited for identifying causal relationships. Nonetheless, these methods might encounter challenges in handling large datasets and maintaining predictive accuracy (Mannering, 2018).

Given this, the objectives of the current study are fourfold: (a) to explore the internal relationship between speed differences and crash risk of RE crashes; (b) to develop data-driven methods for analyzing the injury severity outcomes of both drivers in two-vehicle RE crashes; (c) to compare the predictive performance and goodness-of-fit of data-driven methods with heterogeneity models; (d) to explore the differences in addressing issues of causality and unobserved heterogeneity among approaches of data-driven and heterogeneity models. Thus, the current study fills the knowledge gap by comparing the prediction performance among separate and joint models. Moreover, both statistical and data-driven methods are utilized to explore the significant variables affecting both drivers in rear-end crashes. Lastly, the effects of significant variables, particularly speed differences, on injury severity outcomes have been explored using marginal effects and SHAP approaches.

Fig. 1 shows the methodology of the current study, which commences with a review of recent research on the crash risk associated with RE and examines related works in multi-task learning. Then, an overview of the methodological approaches employed are introduced, along with the dataset. Subsequently, the outcomes of the joint random parameter (RP) models and the cross-stitch multilayer perceptron network (CS-MLP) are compared and analyzed. The paper concludes by interpreting the significance of the findings and their implications and offers recommendations for future research directions.

2. Literature review

2.1. Related works on crash risk of rear-end crashes

Currently, a comprehensive array of research has investigated the risk and outcomes of RE crashes employing diverse methodologies (Abdel-Aty and Abdelwahab, 2004; Harb et al., 2007; Ma et al., 2024; Pande and Abdel-Aty, 2008; Wang and Abdel-Aty, 2006; Wang et al., 2022b; Wu et al., 2020; Wang et al., 2024), while Table 1 states several valuable literature works. Numerous significant discoveries have emerged, emphasizing the critical influence of speed elements on the risk of RE crashes. For example, Das and Abdel-Aty (2011) noted that crashes at higher speeds are more likely to result in severe outcomes. Similarly, Wang et al. (2022a) indicated that elevated vehicle speeds have uniformly resulted in more severe injuries. Furthermore, further in-depth investigation is warranted to examine the interactions between the speed differential of following and leading vehicles and the severity of injuries in RE crashes.

To deal with unobserved heterogeneity, statistical methods, including generalized estimating equations, RP logit/ordered probit models, and joint bivariate probit models, have been developed. Concurrently, data-driven methods, including Bayesian networks, neural networks, and classification trees have also been advanced. Otherwise, some scholars compared the two methods using the same RE

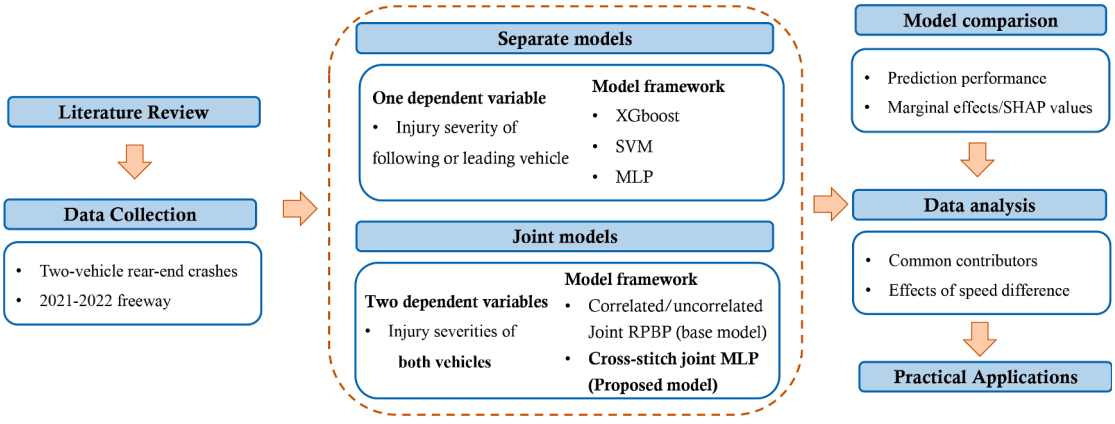

Fig.1. Research tasks of the study.

Table 1
A summary of findings regarding crash risk of rear-end crashes.[a]

Method type	Reference	Methods	Data Source	Sample size	Findings
Statistical methods	Qi et al. (2013) (Work Zones)	Truncated count data and ordered PM	New York 1994 – 2001	2,481	Work zones related to capacity and pavement were associated with the highest frequency compared to other types of work zones. RE crashes associated with alcohol, night, pedestrians, and roadway defects were more severe.
	Wang et al. (2022a) (RE versus non-RE crashes)	RP logit model with heterogeneity in means and variances	Jiangsu Province 2017 – 2019	2,251	Bridge has a higher probability of minor injury and higher risk propensity for fatal injury non-RE crashes in winter was found. The higher operating speeds of cars consistently resulted in more severe injuries. The probability of minor, severe, and fatal injury RE crashes increased with the higher speed difference of cars with adjacent segments in 2019.
	Zou et al. (2023) (Two-vehicle)	Latent class multinomial logit model	Washington State 2010–2016	23,099	The risk factors of curved and sloping road conditions, drivers not wearing seatbelts, and drivers aged 65 and above significantly increase the likelihood of driver fatalities and serious injuries. These three factors contribute to the overall risk from different latent classes.
	Wang et al. (2024a) (Freeway)	Correlated joint RPBP model	Florida State 2019–2021	41,597	There is a positive correlation between the speed differences of leading and following vehicles and the outcomes of injury severity. Leading vehicles' male drivers typically decrease the probability of injury/fatality outcomes across all rear-end crash scenarios. The findings highlight the potential interplay among various factors affecting the injury levels for the drivers.
Data-driven methods	Pande and Abdel-Aty (2006) (Freeway)	Multilayer perceptron (MLP), neural networks	Florida State 1999–2003	2,179	The strategy can potentially identify almost 75 % of RE crashes, with reasonable false alarms. Average speed and occupancy at stations downstream of the crash location were significant as were off-line factors such as the time of day and presence of an on-ramp in the downstream direction.
	Chen et al. (2015) (Highway)	Logit and BN models	New Mexico 2010–2011	11,383	The proposed hybrid approach performs reasonably well. The BN reference analyses indicate that factors, including truck involvement, inferior lighting conditions, windy weather conditions, and the number of vehicles involved could significantly increase driver injury severities in RE crashes.
	Chen et al. (2016) (Highway)	DTNB hybrid classifier	New Mexico 2010–2011	11,383	The presence of heavy vehicles in RE crashes significantly raises the likelihood of driver fatalities, while motorcycle involvement plays a notable role in forecasting driver injuries and fatalities. Fatalities among drivers are more prone to happen in conducive traffic conditions, including clear weather, level road grades, paved surfaces, and particularly on rural roads, with a higher incidence on rural two-lane highways.
	Stylianou and Dimitriou (2018) (Urban network)	BN	Nicosia in Cyprus 2016	317 conflicts	The likelihood of rear-end conflicts may rise under certain conditions: when the involved vehicles differ in type, the speed of the following vehicle exceeds that of the leading vehicle, individual vehicle speed is high with minimal headway, there is a high coefficient of variation in speed values, the nearest intersection type to the measurement point is a priority intersection, the carriageway features a dual design, and conditions are rainy.
Both statistical and data-driven methods	Ahmadi et al. (2020) (Highway)	Multinomial logit, RP logit, and SVM	California state 2007 – 2011	9,468	The SVM approach maintained a slightly better prediction accuracy using the test data. Driving with involvement of alcohol tends to cause more serious outcomes than speeding. Older and male drivers are more likely to have a fatal crash whereas complaint of pain is observed more among female drivers compared to males. Driving in foggy and mountainous or rolling terrains is associated with more fatal and severe injury crashes.
	Moussa et al. (2022) (Highway)	Deep residual neural network and OLR model	North Carolina 2010 – 2017	384,869	The deep residual neural network demonstrated an overall accuracy of 83 %, outperforming the OLR model. Furthermore, the injury severity of drivers involved in rear-end crashes has been found to correlate with the posted speed limit.
	Owais et al., 2024 (Highway)	Deep residual neural network with global sensitivity analysis	North Carolina 2011–2018	96.659	These deep learning layers enable the architecture to gradually deduce high-level information and latent relationships from the supplied data. Using multiple global sensitivity analysis tools is necessary to ascertain the sensitivity analysis conclusions, as no single analytical tool can validate the results.
	Current study (Freeway, two-vehicle)	Correlated RP bivariate PM and CS-MLP model with combined injury severities of the leading-following vehicles	Florida 2021–2022	15,980	The comparative analysis of performance demonstrates the superior predictive capability of MLP network over statistical models. The SHapley Additive exPlanations (SHAP) values reveal that the minimal adverse effects on injury severity for both following and leading vehicles occur with a Δv of 0 to 10 mph, consistent with the pattern observed in the percentage of injury/fatality in RE crashes across Δv.

[a] Note: BN = Bayesian network, DTNB = Decision table/Naïve Bayes, FARS = Fatality Analysis Reporting System, OLR = ordered logistic regression, PM = probit model, RE = rear-end, RP = Random parameters, SHAP = SHapley Additive exPlanations, and SVM = Support vector machine.

crashes dataset. For instance, Ahmadi et al. (2020) found that the SVM approach achieved marginally higher prediction accuracy with the test data. Moussa et al. (2022) stated that the deep residual neural network reached an overall accuracy of 83 %, demonstrating superior performance in comparison to the ordered logistic regression model. To the best of the author's knowledge, a limited scope of literature explores the injury levels for both drivers in following and leading vehicles from a comprehensive aggregate perspective, recognizing the potential interrelationship between them. Furthermore, Mannering et al. (2020) suggest that the choice of data-analysis techniques is made without fully considering the balance between predictive power and the capacity to identify the underlying causal factors leading to crashes. With this in mind, the present paper enhances existing knowledge by comparing the efficacy of statistical and data-driven approaches in analyzing the injury severity outcomes for both drivers in a two-vehicle RE crash.

2.2. Related works of multi-task learning

Joint models can take the same inputs to jointly tackle multiple tasks. Compared to separate modeling for each individual task, joint models can learn the shared features/representations between different tasks, thereby mining shared impacts of variables to different targets to improve the model performance for each task. Although several statistics and econometric models have been proposed to solve joint modeling issue, they rely on specific assumptions (e.g., the task parameter should lie close to each other) and struggle to capture the complex, non-linear relationships in data (Egger et al., 2021; Han et al., 2024), making them less effective for multi-task processing that requires complex feature extraction (Liu et al., 2022; Tan et al., 2022). To mitigate this issue, multi-task learning approaches based on deep neural networks were proposed. Leveraging the powerful non-linear representation capabilities of DL models, this approach can offer more scalability and flexibility in analyzing multiple tasks and achieve higher accuracy (Nweke et al., 2018; Wang et al., 2024b). This advantage is particularly evident in scenarios involving high-dimensional data or intricate interdependencies among variables (Schulz et al., 2020).

In the early multi-task learning approaches, hard parameter sharing approach were widely used, in which the model parameter set is categorized into shared and task-specific parameters (Abdulnabi et al., 2015; Kokkinos, 2017; Vandenhende et al., 2021). Specifically, several DL networks use one common network to learn the shared parameters and then conduct prediction on each sub-network with task-specific parameters. For instance, Kokkinos (2017) introduced the hard parameter sharing model, UberNet, designed to simultaneously address various low-, mid-, and high-level vision tasks. Long et al. (2017) developed a multilinear relationship network to adaptively learn the multilinear relationships of features, classes, and tasks, thus effectively improve the task performance. However, such methods suffer the trade-offs amongst different combinations of shared and task-specific representations (Vandenhende et al., 2021). Besides, extensive experiments are required to determine the optimal network architecture (Misra et al., 2016). To alleviate such issues, Cross-stitch networks introduced soft parameter sharing strategies for multi-task learning (Misra et al., 2016). Rather than employing common networks or parameters, soft feature fusion utilizes linear combinations of parameters in each layer of the task-specific networks. Consequently, individual parameters are allocated to each task, and a feature-sharing mechanism facilitates communication across tasks. Following this, numerous studies utilized and modified such cross-stitch models for multi-task training and achieved outperformed results than other frameworks (Beljaards et al., 2020; Paka et al., 2021; Zhang et al., 2023). For instance, Beljaards et al. (2020) applied such cross-stitch units to connect networks for image registration and segmentation, achieving performance superior to single-task networks. Paka et al., (2021) further enhanced this approach by using cross-stitch modules for shared representation learning to promote network accuracy and robustness. Luo et al (2023) combined the cross-stitch method and co-attention transformer for fault diagnosis in rolling machinery. The experimental outcomes highlighted its superior performance in diagnostic accuracy and adaptability.

In this study, the cross-stitch networks were utilized to jointly analyze the contribution factors of crash severities of following and leading vehicles in RE crashes. Additionally, statistical methods and separated modeling methods were also employed to compare the estimations from the developed cross-stitch deep learning networks.

3. Data description

The data were sourced from two-vehicle RE crashes on interstate freeways in Florida, spanning a two-year interval from January 1, 2021, to December 31, 2022. The dataset contains detailed elements on the injury severity outcomes for both drivers, along with extensive data on demographics, vehicle characteristics, roadway information, environment conditions, and the collision time. Furthermore, the operating speeds of both vehicles at the moment of the crash were determined by the police using various methods (Brach et al., 2022). These methods included the analysis of skid marks, braking distances, vehicle data recorders, assessments of vehicle damage, and time–space analysis (Knill and Fawcett, 1981). As illustrated in Fig. 2, the speed difference (Δv) at the time of impact was quantified.

The dataset includes 15,980 two-vehicle RE crashes, where the severity of driver injuries is reported as fatality, injury, and no injury (property damage only). Due to the small percentages of fatalities (only 0.29 % and 0.11 % for drivers of leading and following vehicles, respectively), the fatality and injury classifications have been combined into one class referred to as Injury/Fatality. Consequently, there were 2,445 injuries/fatalities in following vehicles, compared to 2,686 injuries/fatalities observed in leading vehicles.

As depicted in Fig. 3, significant differences can be observed in the distribution of injury levels for the two vehicles across different speed difference ranges. The observed injury severity outcomes of RE crashes, attributed to Δv ranging from [5, 10) mph, are the lowest across all examined ranges. In addition, the injury severity outcomes become serious with the increase of Δv ranging from 5 mph, while it achieves the most severe injury outcomes at almost 20 % injury/fatality rate for Δv of no less than 25 mph. This phenomenon is interesting as the lowest injury severity levels are not at the Δv range of [0, 5] mph, but in the Δv range of [5, 10) mph, which shaped like the Solomon Curve indicated by Solomon (1964) and Hauer (1971).

In each subgroup, there are more severe outcomes for the leading vehicles. This finding could be explained by the fact that drivers in the leading vehicle typically have less time to react or prepare for impact compared to those in the following vehicle, affecting their readiness and the severity of potential injuries. Moreover, the striking force with more energy is preferred to transfer from the following vehicle to the leading vehicle, exposing drivers of leading vehicles to a sudden and unexpected forceful impact. This results in a significant break in vehicle movement, increasing the propensity of suffering injury or fatality. However, the shift in injury severity outcomes from the following vehicle to the leading vehicle is most pronounced for a Δv of [10, 15) mph, at 3.28 %, while the shift for [25, $+\infty$) mph is the smallest, at 0.41 %. Moreover, distinct differences also exist in the total numbers of RE crashes for various Δv ranges. There are 2,388 RE crashes caused by Δv of [5, 10)

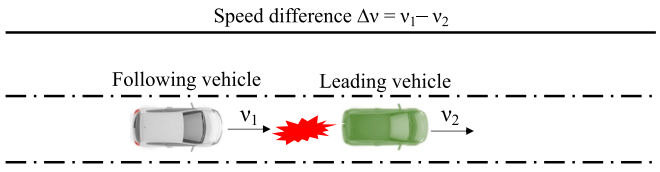

Fig.2. Speed difference between leading (struck) and following (striking) vehicles in RE crashes.

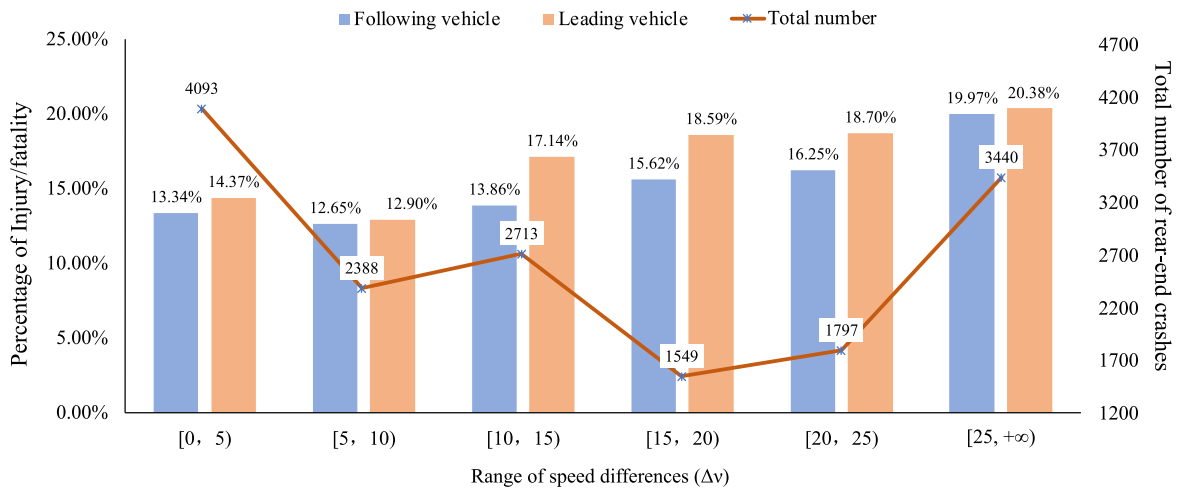

Fig.3. Injury/Fatality percentage and total number of RE crashes across speed difference (Δν).

mph, lower than the number caused by Δν of [0, 5) and [10, 15) mph.

Otherwise, the mean values for the explanatory variables are displayed in Fig. A1, including the driver, vehicle, roadway, environment, crash and time attributes.

4. Methodology

To analyze the injury severity outcomes and the influencing factors of two vehicles involved in a crash, two joint models were developed including joint RP bivariate probit models (correlated and uncorrelated joint RPBP models, statistical model) and a cross-stitch multilayer perceptron network (CS-MLP, deep learning model). Moreover, the separate models were also estimated to compare the predictive measures of separate and joint frameworks, to highlight the superiority of joint models in capturing unobserved heterogeneity and correlated errors existing in the aggregate levels.

4.1. Correlated joint RPBP model

To address the issue of unobserved heterogeneity in two-vehicle RE crashes, factors that vary across observations (known as random parameters, RPs), the correlations among these RPs, and other factors influencing the means of these RPs need to be comprehensively considered. To this end, a correlated joint RP bivariate probit model, which can account for heterogeneity in means, was employed to investigate the factors influencing the injury severity outcomes of both drivers. Following with Washington et al. (2020), the bivariate probit model is detailed as follows,

$$\boldsymbol{Y}_{i,1} = \beta_{i,1}\mathbf{X}_{i,1} + \varepsilon_{i,1}, s_{i,1} = 1 if S_{i,1} > 0, 0 otherwise$$

$$\boldsymbol{Y}_{i,2} = \beta_{i,2}\mathbf{X}_{i,2} + \varepsilon_{i,2}, s_{i,2} = 1 if S_{i,2} > 0, 0 otherwise \quad (1)$$

Consider a bivariate normally distributed the error terms $\boldsymbol{\varepsilon} = \begin{pmatrix} \varepsilon_{i,1} \\ \varepsilon_{i,2} \end{pmatrix}$ by following,

$$N\left[\begin{pmatrix} 0 \\ 0 \end{pmatrix}, \begin{pmatrix} 1 & \rho \\ \rho & 1 \end{pmatrix}\right] \quad (2)$$

The vector **X** are explanatory factors to driver's injury severity outcomes in RE crashes, with the vector β denoting their corresponding estimable parameters. The two binary outcomes $s_{i,1}$ and $s_{i,2}$ represent the injury severities of the following and leading vehicles, respectively, while $Y_{i,1}$ and $Y_{i,2}$ are their corresponding latent variables. Assuming the errors $\varepsilon_{i,1}$ and $\varepsilon_{i,2}$ follow a normal joint distribution, they can be characterized by a mean of 0 and a variance of 1. The correlation coefficient ρ is indicative of the cross-equation error correlation. The cumulative bivariate normal distribution function can be expressed as (Bhat, 2018),

$$\Phi(Y_{i,1}, Y_{i,2}; \rho) = \frac{e^{-\frac{(\boldsymbol{Y}_{i,1}{}^2 + \boldsymbol{Y}_{i,2}{}^2 - 2\rho \boldsymbol{Y}_{i,1}\boldsymbol{Y}_{i,2})}{2-2\rho^2}}}{\left[2\pi\sqrt{(1-\rho^2)}\right]} \quad (3)$$

In the bivariate probit model, the probability for $s_{i,1} = 1$ and $s_{i,2} = 1$ can be written as follows (Washington et al., 2020),

$$P(s_{i,1}=1, s_{i,2}=1) = P(\mathbf{X}_{i,1} < \mathrm{x}_{i,1}, \mathbf{X}_{i,2} < \mathrm{x}_{i,2}) = \int_{-\infty}^{\mathrm{x}_{i,1}} \int_{-\infty}^{\mathrm{x}_{i,2}} \Phi(\mathrm{z}_{i,1}, \mathrm{z}_{i,1}; \rho) \mathrm{d}\mathrm{z}_{i,1} \mathrm{d}\mathrm{z}_{i,2} = F(\beta_{i,1}\mathbf{X}_{i,1}, \beta_{i,2}\mathbf{X}_{i,2}; \rho) \quad (4)$$

Based on the maximum likelihood method, the log-likelihood function could be given by (Bhat, 2018),

$$F = \sum_{i=1}^{N} \begin{bmatrix} \boldsymbol{Y}_{i,1}\boldsymbol{Y}_{i,2} ln\Phi(\beta_{i,1}\mathbf{X}_{i,1}, \beta_{i,2}\mathbf{X}_{i,2}, \rho) + (1 - s_{i,1}) s_{i,2} ln\Phi(-\beta_{i,1}\mathbf{X}_{i,1}, \beta_{i,2}\mathbf{X}_{i,2}, -\rho) \\ +(1 - s_{2,1}) s_{i,1} ln\Phi(\beta_{i,1}\mathbf{X}_{i,1}, -\beta_{i,2}\mathbf{X}_{i,2}, -\rho) \\ +(1 - s_{i,1})(1 - s_{i,2}) ln\Phi(-\beta_{i,1}\mathbf{X}_{i,1}, -\beta_{i,2}\mathbf{X}_{i,2}, \rho) \end{bmatrix} \quad (5)$$

Furthermore, to capture the multilayer unobserved heterogeneity, the model incorporates β_n, as defined in Mannering et al. (2016),

$$\beta_i = b + \lambda \boldsymbol{Y}_i + \mathbf{C}\delta_i \quad (6)$$

where $\boldsymbol{b}$ represents the average estimable parameter across the crashes. Through the estimable parameters λ, the explanatory variables S_i would affect the mean of the parameter β_i. While **C** is a Cholesky matrix to define the covariances matric for the RP, and δ_i denotes a disturbance

term characterized by a mean of 0 and a variance of σ^2.

As for the standard deviation of the correlated RP (Ahmed et al., 2021; Fountas et al., 2018):

$$\sigma_r = \sqrt{\sum_{k=1}^{l} \sigma_{l,k}{}^2} \tag{7}$$

where σ_r denotes the standard deviation of the random parameter r, with $\sigma_{l,l}$ being the diagonal elements of the Γ matrix, and $\sigma_{l,l-1}$, $\sigma_{l,l-2}$, …, $\sigma_{l,1}$ are the off-diagonal elements of the lower triangular matrix.

The mean standard error and the corresponding t-statistic of σ_r are calculated as follows (Fountas et al., 2018):

$$Mean_{\sigma_r} = \frac{S_{\sigma_m}}{\sqrt{N}} \tag{8}$$

$$Stat_{\sigma_r} = \frac{\sigma_r}{SE_{\sigma_r}} \tag{9}$$

where S_{σ_m} is the standard deviation of σ_{rn} and N is the observation number. Then, the covariance of two RPs can be estimated (Fountas et al., 2021):

$$Covariance\left(\chi_{m1,n}, \chi_{m2,n}\right) = \frac{covariance\left(\chi_{m1,n}, \chi_{m2,n}\right)}{\sigma_{m1,n}\sigma_{m2,n}} \tag{10}$$

where, $m1$ and $m2$ are the correlated RP while $\sigma_{m1,n}$ and $\sigma_{m2,n}$ denote their standard deviations.

Balancing the trade-off between estimation performance and computational efficiency (McFadden and Train, 2000), 1000 Halton draws are simulated through maximum likelihood method. As for the distribution of random parameters, the normal distribution has been identified as providing the most appropriate statistical fit (Milton et al., 2008; Behnood and Al-Bdairi, 2020).

Then, the marginal effects E on $j-th$ RE crash injury could be determined as follows (Christofides et al., 1997; Greene, 2012),

$$\begin{aligned} ME_{S_{i,1}} &= \overline{P_j\left(s_{i,1}, s_{i,2}\right)}\left[given \mathbf{X}_{i,1} = 1\right] - \overline{P_j\left(s_{i,1}, s_{i,2}\right)}\left[given \mathbf{X}_{i,1} = 0\right], \\ ME_{S_{i,2}} &= \overline{P_j\left(s_{i,1}, s_{i,2}\right)}\left[given \mathbf{X}_{i,2} = 1\right] - \overline{P_j\left(s_{i,1}, s_{i,2}\right)}\left[given \mathbf{X}_{i,2} = 0\right] \end{aligned} \tag{11}$$

4.2. Cross-stitch multilayer perceptron network

The CS-MLP model is one kind of multi-task deep learning models which can investigate the correlations of two tasks and extracting their shared features to improve each model performance. For one RE crash, common factors (e.g., vehicle characteristics, environmental features, and traffic status, etc.) would affect both drivers' severities in different degree. Therefore, it can be seen as a two-task problem (i.e., jointly evaluating the crash severities of the drivers in leading (task 1) and following vehicle (task 2)). Given the inherently connection between these two tasks, the jointly modeling through the CS-MLP could provide more precise estimations of the correlations between such features with crash severities rather than modeling separately in previous studies (Misra et al., 2016).

4.2.1. Overall model structure

The overall structure of the proposed CS-MLP model is illustrated in Fig. 4. Given the model inputs X, two MLP network A and B were developed for evaluate the injury severity for following vehicle Y_1 and leading vehicle Y_2. The two networks have the same network structure with 4 fully connected (FC) layers of 128, 64, 32, and 32 dimensions, respectively. In the first three FC layers, the model parameters F_i of the two networks were connected through cross-stitch units to generate their shared parameters SF_i, which are then passed into the next FC layer. By combining network parameters in the cross-stitch units, both tasks can be regularized to learn and enforce shared representations with each other. Therefore, the network A could get direct supervision from the severity evaluation task for following vehicle and indirect supervision (through cross-stitch units) from another severity evaluation task for leading vehicle. Similarly, the network B could also get the knowledges from both tasks through cross-stitch units. Finally, the features of last FC layer of both networks are transformed through a sigmoid function to predict the final crash severity label for leading vehicle $\widehat{Y_1}$ and following vehicle $\widehat{Y_2}$.

4.2.2. Cross-stitch units

The cross-stitch approach was proposed by Misra et al. (2016) to learn shared representations from multiple deep-learning tasks. Consider a case of multi-task learning with two networks for tasks A and B, the cross-stitch unit can combine their model parameters and determine how much sharing is needed for each task based on specific weights. Fig.5 presents the feature-sharing process in a cross-stitch unit, in which the shared features are calculated by learning a linear combination of the input features. Given x_A, x_B denotes the features from two

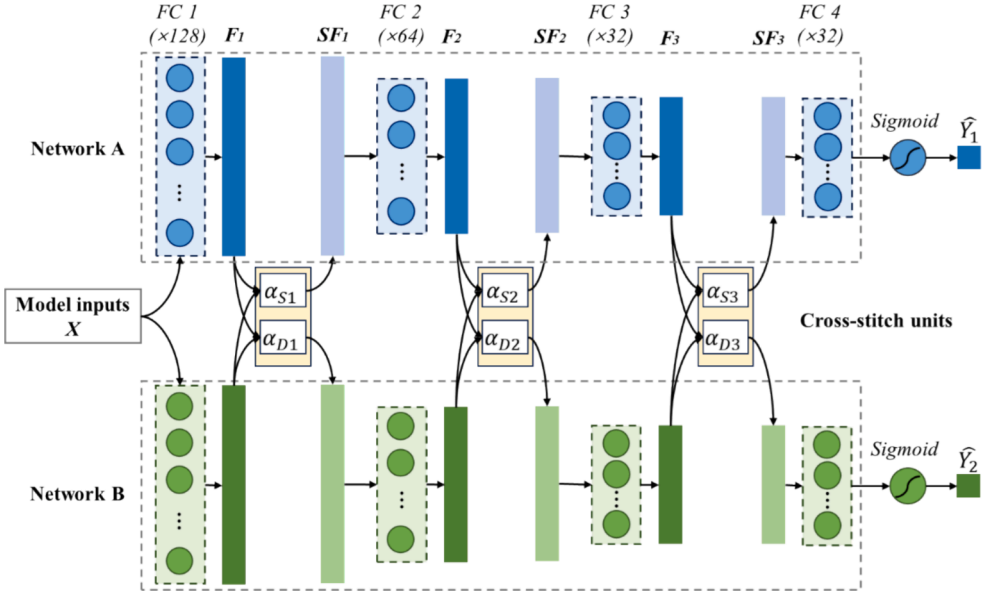

Fig.4. Structure of the CS-MLP model.

task A and B, the linear combinations $\widetilde{x}_A$, $\widetilde{x}_B$ of both input task features are learned and feed as input to the next layers. This linear combination is parameterized using α. Specifically, at location (i,j) in the networks, the linear combinations $\widetilde{x}_A^{ij}$ and $\widetilde{x}_B^{ij}$ can be calculated by:

$$\begin{bmatrix} \widetilde{x}_A^{ij} \\ \widetilde{x}_B^{ij} \end{bmatrix} = \begin{bmatrix} \alpha_{AA} & \alpha_{AB} \\ \alpha_{BA} & \alpha_{BB} \end{bmatrix} \begin{bmatrix} x_A^{ij} \\ x_B^{ij} \end{bmatrix} \tag{12}$$

Though such cross-stitch operation in each layer, the network can dynamically adjust the sharing weights to either specialize certain layers by setting α_{AB} or α_{BA} to zero or promote a more shared representation by assigning a higher value to them, as shown in Fig. 5.

As for the backpropagating through cross-stitch units, since they are modeled as linear combinations, their partial derivatives for loss L with tasks A, B are easy to compute as:

$$\begin{bmatrix} \frac{\partial L}{\partial x_A^{ij}} \\ \frac{\partial L}{\partial x_B^{ij}} \end{bmatrix} = \begin{bmatrix} \alpha_{AA} & \alpha_{AB} \\ \alpha_{BA} & \alpha_{BB} \end{bmatrix} \begin{bmatrix} \frac{\partial L}{\partial \widetilde{x}_A^{ij}} \\ \frac{\partial L}{\partial \widetilde{x}_B^{ij}} \end{bmatrix} \tag{13}$$

$$\frac{\partial L}{\partial \alpha_{AB}} = \frac{\partial L}{\partial \widetilde{x}_B^{ij}} x_A^{ij}, \frac{\partial L}{\partial \alpha_{AA}} = \frac{\partial L}{\partial \widetilde{x}_A^{ij}} x_A^{ij} \tag{14}$$

The α_{AB}, α_{BA} are denoted by α_D, the different task values as they weigh the activations of another task. Likewise, α_{AA}, α_{BB} are denoted by α_S, the same-task values since they weigh the activations of the same task. The values of α_D and α_S are initialized with specific values (e.g., 0.1 and 0.9) and automatically varied during the model training. Therefore, the unit can freely move between shared and task-specific representations and choose a middle ground if needed.

4.2.3. Objective loss function

For the jointly CS-MLP model, the objective is to minimize the combined loss of the two tasks. Given these two tasks are binary classification problems, the cross-entropy loss between the model outputs and the real crash severities was used as L_A and L_B:

$$LOSS = -\frac{1}{N}\sum_{k=1}^{N} y^k \log(p^k) + (1-y^k)\log(1-p^k) \tag{15}$$

where N is the total number of samples, p^k is the output probability of network for the k-th sample, y^k is the true crash severity label.

Therefore, the final loss function is the weighed combination of L_A and L_B:

$$L = w_A L_A + w_B L_B \tag{16}$$

where w_A, w_B are the weights for L_A, L_B, respectively. It is worth noting that the weights are set as two trainable parameters with an initial value of 0.5, which allows the network to take a balance of the two losses to achieve the best model performance.

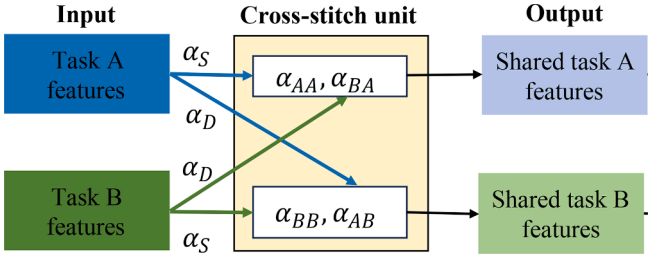

Fig.5. Illustration of the cross-stitch unit.

4.2.4. Shapley Additive exPlanations (SHAP) approach

Unlike the statistical model, the MLP cannot directly provide the quantified impacts of input variables on the targets. Therefore, the widely used SHapley Additive exPlanations (SHAP) approach (Lundberg and Lee, 2017) is employed to explain the results of the proposed CS-MLP model. SHAP can be seen as a post-hoc explanation method based on game theory (Štrumbelj and Kononenko, 2014) and local explanations (Ribeiro et al., 2016). In SHAP, the contribution of each feature to the model output $v(N)$ is allocated based on their marginal contribution. For a feature i, its shapely values $\varnothing_i$ can be represented by:

$$\varnothing_i = \sum\nolimits_{S \in N} \frac{|S|!(|N|-|S|-1)!}{|N|!} [v(S \cup \{i\}) - v(S)] \tag{17}$$

where N is the set of all model features, $S \in N$ are all possible subsets of features without i.

5. Results and discussion

The current study utilizes both statistical and data-driven methods to investigate the advantages of joint models over existing separate models.

In terms of statistical methods, the correlated joint RPBP model is developed. To assess the predictive performance of such an estimated model, the k-fold cross-validation method was employed. Given the sample size and computational constraints, k is determined to be five, resulting in the random division of the 15,980 observations into five subsets (5*3196). For each of the estimated models, both the model estimation and validation processes are repeated five times. During each iteration, four of the five subsets (serving as training data) are utilized for parameter estimation, while the remaining subset (serving as testing data) is employed to compute the evaluation metrics for prediction accuracy. Following this procedure, the evaluation metrics from the five testing subsets are aggregated to derive the final predictive performance results.

Otherwise, three widely used data-driven models, including Support Vector Machines (SVM), eXtreme Gradient Boosting (XGBoost), and MLP are also developed as separate models (baseline). For the separate MLP models, they share the same network structure as networks in CS-MLP (i.e., 4 fully connected (FC) layers of 128, 64, 32, and 32 dimensions respectively and a sigmoid layer). The only difference is that they were not connected by cross-stitch units. Therefore, the benefits of the cross-stitch units can be explored through the comparison of two separate MLP models and the CS-MLP.

5.1. Model performance comparison

In terms of the prediction metrics, accuracy, recall, false alarm rate (FAR), F-1 score, and the Area Under ROC Curve (AUC) are used, which can be calculated by:

$$Accuracy = (TP+TN)/(TP+TN+FP+FN) \tag{18}$$

$$Recall = TP/(TP+FN) \tag{19}$$

$$FAR = FP/(TN+FP) \tag{20}$$

$$F-1\ score = TP/(TP+0.5(FP+FN)) \tag{21}$$

Among them, accuracy represents the overall ratio of correctly classified samples to all samples, while it may not accurately reflect the prediction performance under such an imbalanced dataset in this study; Therefore, recall, the FAR and F-1 scores were also utilized. Recall means the ratio of correctly classified positive samples (the injury crashes) and FAR means the ratio of correctly classified negative samples (the non-injury crashes); the F-1 score is the harmonic mean of sensitivity and precision, which can reflect the comprehensive classification accuracy under unbalanced datasets. The calculation of the above

four metrics needs a confusion matrix with a specific classification threshold, as shown in Table 2. In this study, the classification threshold in each model is determined according to the FAR to make sure that other metrics can be compared at the same FAR level (0.2). Therefore, other metrics can be compared at the same FAR level. As for AUC, it measures the area under the Receiver Operating Characteristic curve under the classification threshold from 0 to 1. The higher the AUC, the better the model is at distinguishing between the two classes.

Table 3 presents the prediction performance of different models on the test dataset. From the results, the main points can be summarized:

(1) In both tasks, the CS-MLP model has achieved better prediction performances than others. Specifically, for the crash severity evaluation of the following vehicle, the proposed CS-MLP provides the highest accuracy of 0.754 and F1 score of 0.399, followed by the separate MLP. In addition, the CS-MLP shows the highest AUC of 0.726, indicating it has the best model overall performance. The same trend is also seen in the task of crash severity evaluation of leading vehicles. The CS-MLP had the highest sensitivity of 0.425, F1 score of 0.330, and AUC of 0.671. Compared with separately trained MLP models, the CS-MLP could improve the model recall at 6.67 % (equal to (0.528–0.495)/0.495) and 5.99 % (equal to (0.425–0.401)/0.401) at Tasks 1 and 2. It demonstrates that the cross-stitch units could automatically fit the shared weights, thereby extracting the useful features from another task to improve its own model outputs.
(2) The model performance of the correlated joint RPBP is not as good as other machine learning models, which is consistent with existing research (Moussa et al., 2022). It shows the better prediction ability of ML models than the statistical models. Among the ML models, the MLP shows better recall, F-1 Score, and AUC than the SVM and XGBoost models. It indicates that the fully connected networks in MLP models can better capture the relationships between the crash influence factors and crash severity based on their powerful non-linear fitting capabilities.
(3) The overall model performances at the first task, evaluating the crash severity of the following vehicle, are better than that of task 2 for leading vehicles. It could be explained by the fact that in an RE crash, the driver in the following vehicle is much closer to the crash position (the front of the vehicle) and thus directly bears the possible injuries caused by the crash. Therefore, the crash severity of the drivers in the following vehicle would be more closely related to their contribution factors (e.g., the crash type, involved vehicle type, etc.) compared to the leading vehicles.

5.2. Model results interpretation

5.2.1. Correlated joint RPBP model results

Table A1 shows the model results for the freeway two-vehicle RE crashes across 2021–2022 based on the correlated joint RPBP model. The model estimation yielded a high corrected ρ^2 value and a ρ-value of 0.298 and 0.612, respectively, in contrast to the uncorrelated joint model, which recorded indices of 0.291 and 0.588. Eight indicators are observed to affect the injury severity outcomes of both vehicles, such as indicators of V1 truck, V2 passenger car, speed difference, and daytime. Fig. 6 displays the marginal effects of the 8 common variables affecting the injury severity of both vehicles in the correlated joint RPBP model.

Table 2
Confusion matrix for crash severity classification.

True Condition	Prediction Result	
	Injury crash	No injury crash
Injury crash	True Positive (TP)	False Negative (FN)
No injury crash	False Positive (FP)	True Negative (TN)

Interestingly, it could be found that both the V1 truck and V2 passenger car decreased the injury severity outcomes of the following vehicle while increasing that of the leading vehicle (Fig. 6 (a, b)). The possible reason might be the differing mechanisms in RE crashes striking or being struck by passenger cars and trucks. Furthermore, an increase in the speed difference was observed to elevate the injury severity outcomes for both following and leading vehicles, with marginal effects of 0.0041 and 0.0026, respectively, as shown in Fig. 6 (e).

Moreover, three variables are observed to produce random parameters including male driver of following vehicle and level roadway defined for following vehicle and daytime indicator specific to leading vehicle. With a mean (variance) of −0.285 (0.187), male drivers of following vehicles are identified as a random parameter specific to the following vehicle. The normal distribution indicates that 93.6 % of these male drivers would decrease the injury likelihood, while the remaining 6.4 % would increase the injury severity outcomes. This phenomenon could be explained by the greater muscle mass and bone density of the male drivers, enhancing their physical resilience in the rear-end crashes (Nieve et al., 2009). Moreover, level road segments are identified as a random parameter for following vehicles. The normal distribution shows that 80.5 % of following vehicles are associated with a lower injury likelihood in rear-end crashes. For leading vehicles, daytime is identified as a random parameter with a mean (variance) of −0.303 (0.136). This normal distribution shows that 98.7 % of leading vehicles are associated with a lower injury likelihood in rear-end crashes.

Moreover, the elements of the Cholesky matrix for the correlated random parameters are also shown in Table A1, along with the correlation coefficients. Notably, a positive correlation of 0.854 is found among the indicators of level roadway and daytime, characterized by the unobserved heterogeneity interaction among these two random parameters. It indicates RE crashes occurred during daytime at level geometric segments would cause a higher injury/fatality likelihood. The possible reason might be that drivers are more prone to speeding under this circumstance, generating more serious outcomes (Chen et al., 2016; Zeng et al., 2019).

A similar trend is observed between male drivers of the following vehicle and level roadways, showing a positive correlation of 0.696. The heterogeneity identified by the correlation coefficient between these two random parameters attenuates the impacts on the injury outcomes of RE crashes. This interaction suggests compensatory effects on injury levels, as illustrated by the correlation among variations in driver, roadway, and temporal-specific indicators.

Such correlation unveils new perspectives and encourages in-depth investigation into the alternate, unobserved heterogeneity regarding the injury levels for both drivers. This correlation captures such unobserved heterogeneity, which might be overlooked in uncorrelated random parameters in bivariate probit analyses or data-driven methods.

5.2.2. CS-MLP model results

Fig. 7 presents the SHAP summary plots of top-20 important variables for the following vehicle severity in separate MLP and CS-MLP. The results show that although most of important variables are consistent between these two models, there are still some differences in their importance ranking and SHAP value distributions. The most obvious difference is the variable speed difference. In the separate MLP model, speed difference is the fifth important variable and its SHAP value varies between −0.2 and 0.2. While in the CS-MLP, the speed difference becomes the most important variable with larger absolute SHAP values from 0 to 0.4. It means that the key impact of speed difference on crash severity was identified based on the jointly modeling. For other variables, their influences on the following vehicle crash severity are consistent between the separate and joint models. For example, they both show the negative effect of V2 passenger car, which indicates that the crash severities of following vehicles would be more likely to be non-injury if the leading vehicles are passenger cars. Same trends can also be seen for variables of Daytime, V2 rear center bumper, and V1 male. To

Table 3
Prediction performance comparison between separate and joint models.

Crash severity	Model type	Model	Model performance			
			Accuracy	Recall	F-1 Score	AUC
Y_1 for following vehicle	Separate models	XGBoost	0.744	0.409	0.331	0.655
		SVM	0.746	0.489	0.373	0.702
		MLP	0.755	0.495	0.385	0.718
	Joint models	Correlated joint RPBP	0.600	0.523	0.316	0.575
		Uncorrelated joint RPBP	0.594	0.517	0.322	0.569
		CS-MLP	**0.754**	**0.528**	**0.399**	**0.726**
Y_2 for leading vehicle	Separate models	XGBoost	0.733	0.338	0.276	0.612
		SVM	0.742	0.375	0.305	0.652
		MLP	0.738	0.401	0.315	0.653
	Joint models	Correlated joint RPBP	0.545	0.423	0.326	0.590
		Uncorrelated joint RPBP	0.549	0.419	0.313	0.589
		CS-MLP	**0.740**	**0.425**	**0.330**	**0.671**

Note: Uncorrelated joint RPBP model is the base model for correlated joint RPBP model without correlation for the random parameters.

sum up, the results of CS-MLP are almost consistent with that of separate MLP, but the prominent role of speed difference is emphasized.

For the leading vehicle severity analysis, Fig. 8 presents the SHAP summary plots of top-20 important variables in the corresponding separate MLP and CS-MLP. Similarly, most of important variables are consistent while they have different importance ranking and SHAP value distributions in the two models. In the separate MLP model, speed difference is the second important variable, and its SHAP value varies between −0.3 and 0.2. In the CS-MLP, the speed difference becomes the most critical variable with much larger absolute SHAP values from 0 to 0.5. It shows that the speed difference becomes the critical factor in both leading and following crash severity in the joint model. The three variables of V2 male, daytime, and V2 truck, are all identified as the most important variables with negative effects in the two models. It indicates that the crash severities of the leading vehicle trend to be not severe (i.e., non-injury) when the driver in the leading vehicle is male, the crash happens daytime, and the leading vehicle is a truck. Moreover, the importance ranking of variable Clear increases to 5th in CS-MLP from 8th in separate MLP, which means the clear weather is more essential to decrease the likelihood of injury crash for the leading vehicles.

Based on the SHAP results of CS-MLP, the impacts of different variables to crash severities of the involved vehicles can be visualized as shown in the Fig. 9. In the figure, each arrow points from the variable to the crash severity of the vehicle. Its thickness represents the absolute value of its corresponding SHAP value, the degree of impact on the crash severity. The colors of the arrows represent the positive (red) or negative (green) impacts of the variable on the crash severity.

Given the results, 14 common variables are found to affect the crash severities of both drivers in the RE crashes:

(1) The most important variable in the common variables is the speed difference of the two vehicles when crash occurs, which is consistent with the conclusions of existing studies (Das and Abdel-Aty, 2011). The greater the speed difference, the greater the impact force will be endured, resulting in a more severe crash for both vehicles (Wang et al., 2024a). Fig. 10 illustrates the impact of speed difference on the injury severity for both vehicles, as quantified by SHAP values. The SHAP values show a comprehensive phenomenon of effects of speed difference on both the injury severity outcomes. Moreover, the SHAP values of following vehicle are lower than those of leading vehicles. This aligns with the marginal effects measured by the correlated joint RPBP model, indicating average values for effects of 0.0041 and 0.0026 for following and leading vehicles, respectively, shown in Fig. 6 (e).

It is noted that the SHAP values indicating the effect on the injury levels of the following vehicle are positive, except for speed differences ranging from 0 to 15 mph. Regarding leading vehicles, the SHAP values turn negative when the speed difference ranges from 0 to 10 mph. This suggests the least adverse effects on the injury severities within a speed difference of 0 to 10 mph, aligning with the relationship between speed differences and injury severity outcomes presented in Fig. 3. Additionally, this trend also mirrors the Solomon Curve as delineated by Solomon (1964) and Hauer (1971).

Additionally, a notable variation exists in the trend of SHAP values as the speed difference increases. Specifically, once the speed difference surpasses 15 mph, the SHAP values associated with the following vehicle rise alongside the increase in speed difference, indicating a positive correlation between the degree of aggravation and the speed difference. Nonetheless, the SHAP values peak at a speed difference of approximately 20 mph and then gradually decrease as the speed difference exceeds 20 mph. Given this context, the SHAP values derived from the CS-MLP model visually analyze the relationship between speed difference and injury severity outcomes, capturing their non-linear trends. This facilitates the identification and explanation of variable trends within the model and their influence on the prediction.

(2) Six factors related to the following vehicle are observed to be the common factors. Among them, the variable V1 speeding is significantly positive to both vehicles crash severities. It demonstrates the significant hazards of vehicle speeding as it would make both vehicles suffer more power and impact during crash, thereby increasing their crash severity (Zhang and Hassan, 2019). It should be noted that the V1 truck is negative to the crash severity of the following vehicle but positive to that of the leading vehicle. It means although the truck can protect the driver well, it would increase the crash severity of drivers in the following vehicle. This exciting phenomenon was also observed in the correlated joint RPBP model, shown in Fig. 6 (e).
(3) Regarding the factors associated with the leading vehicle, V2 passenger car negatively influences the crash severity of the following vehicle but positively affects that of the leading vehicle. This indicates that if the leading vehicle is a passenger car, the crash severity for the following vehicle is reduced, while it slightly increases for the leading vehicle. Similarly, if the leading vehicle is a truck (V1 truck), it can offer substantial protection to its driver while causing more severe injuries to the drivers in the following vehicle. Furthermore, the old indicator of the V2 vehicle positively impacts the crash severities of both vehicles, highlighting the safety concerns related to older vehicles as they contribute to increased crash severities for both following and leading vehicles. Despite the possibility that the drivers involved may possess considerable driving experience, the risk of injury in RE crashes, especially when colliding with another vehicle, may be heightened due to the insufficient protection provided by older vehicles, as well as their poor mechanical properties and reduced stability .

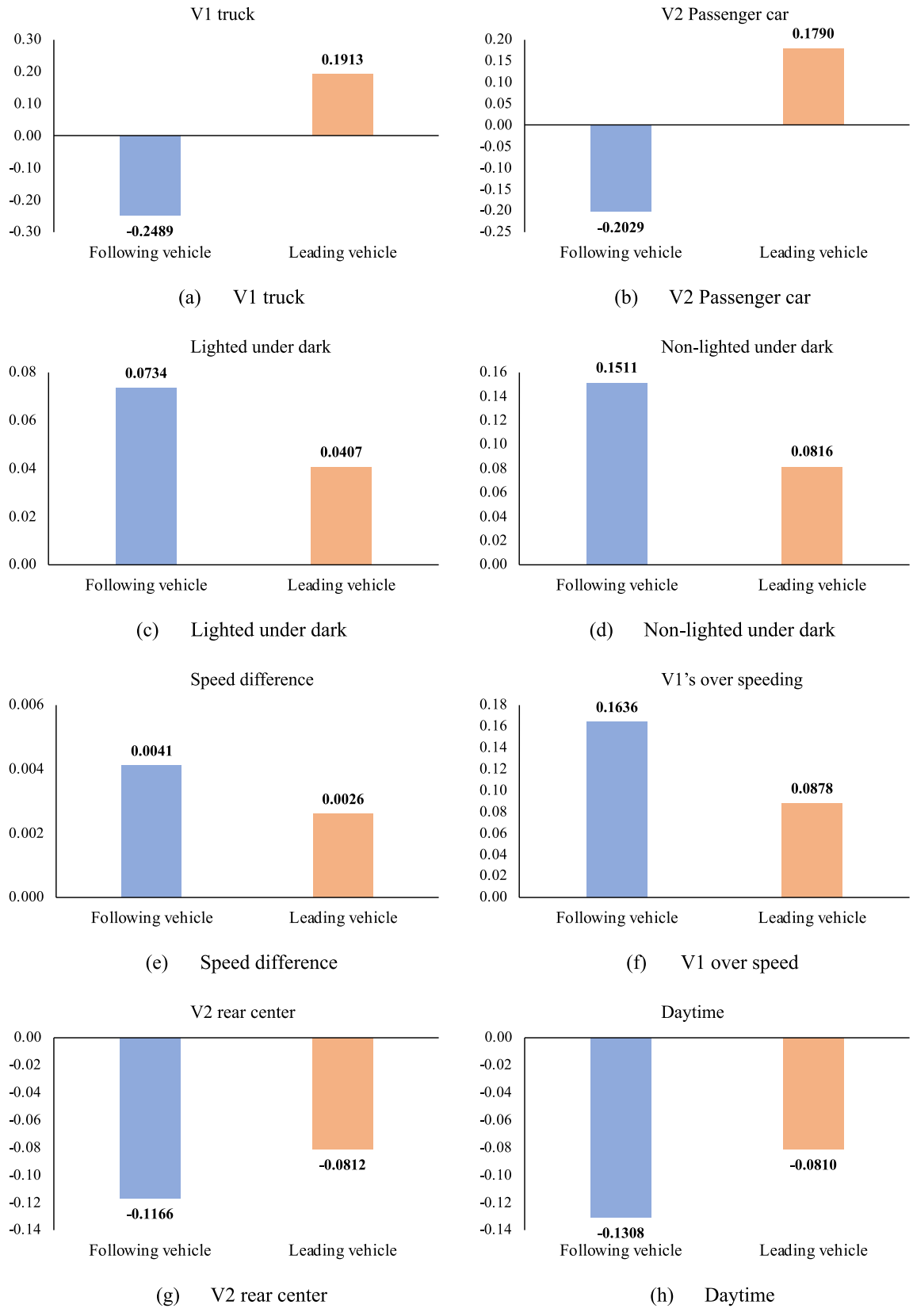

Fig.6. Marginal effects of the common variables affecting the injury severity of both following and leading vehicle in correlated joint RPBP model.

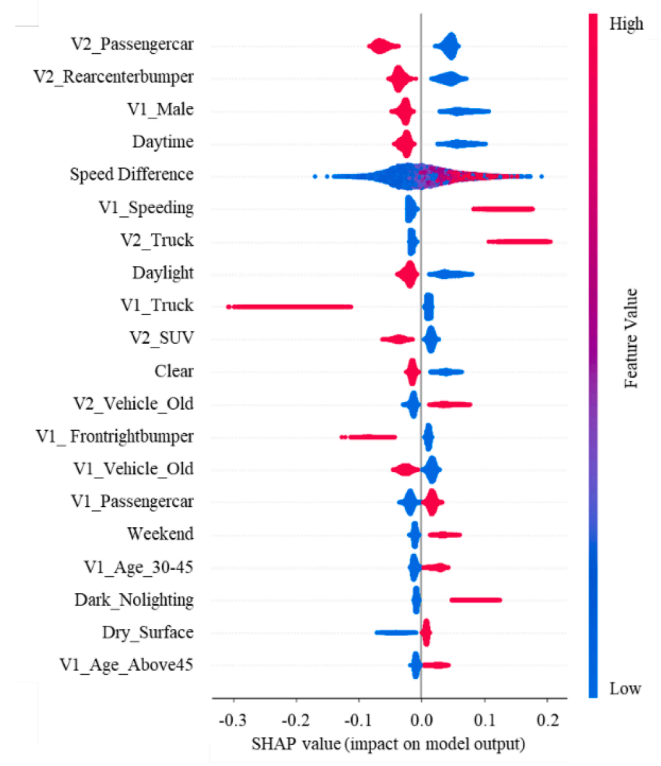

(a) Separate MLP

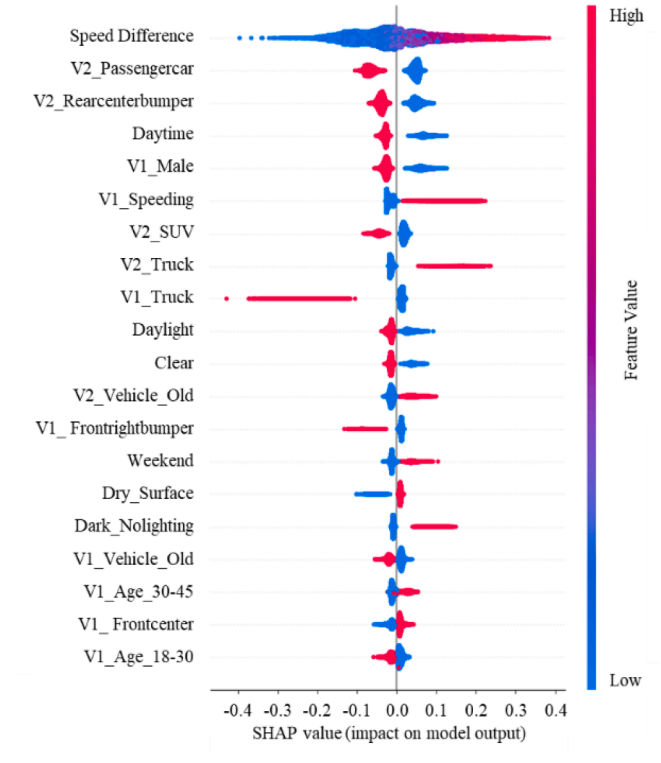

(b) CS-MLP

Fig.7. SHAP summary plots of top-20 important variables for the following vehicle severity.

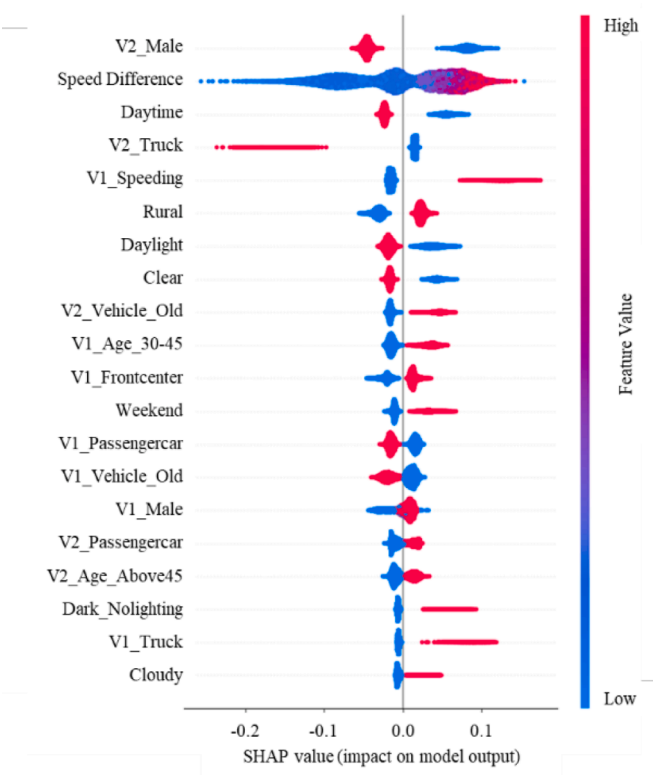

(a) Separate MLP

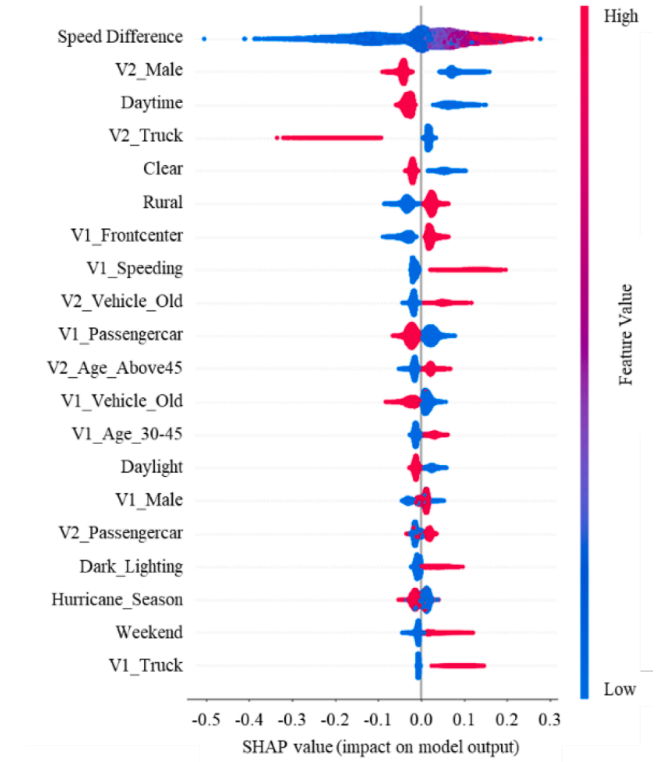

(b) CS-MLP

Fig.8. SHAP summary plots of top-20 important variables for the leading vehicle severity.

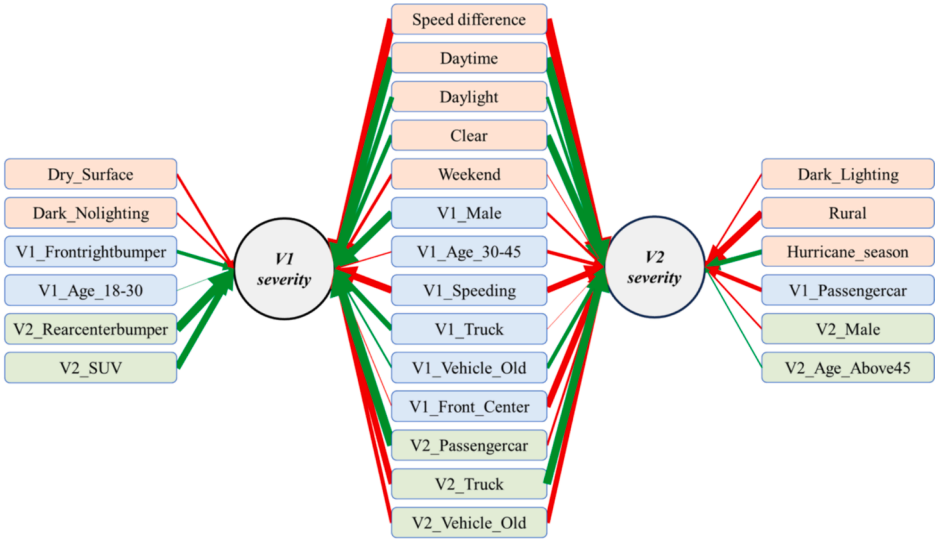

Fig.9. Impacts of different variables to crash severities of the involved vehicles.

(4) Regarding the environmental characteristics, the daytime, daylight, and clear variables negatively impact both vehicles' crash severities. This indicates that under favorable conditions (daytime and clear weather), drivers in the following vehicles benefit from improved visibility before the crash occurrence. Consequently, drivers can implement defensive actions (e.g., slowing down and emergency braking) in advance, thus preventing more severe crashes (Das et al., 2018).

6. Conclusions

To examine the relationship between speed difference among the following and leading vehicles (Δv) and crash risk of RE crashes, correlated joint random parameters bivariate probit model (statistical method) and CS-MLP (data-driven method) are developed. Data of 15,980 two-vehicle RE crashes are collected over a two-year period, from January 1, 2021, to December 31, 2022, divided into two possible injury severity levels of no injury and injury/fatality for both drivers of following and leading vehicles.

The comparative analysis of performance demonstrates the superior predictive capability of CS-MLP over RPBP model. Within these networks, the MLP network outperforms the SVM and XGBoost networks in terms of recall, F-1 Score, and AUC. However, the significant correlation among RP, as identified by the correlated joint random parameters bivariate probit model, effectively captures the unobserved heterogeneity in interactions among key factors influencing injury severity outcomes for both drivers in a single two-vehicle RE crash. Notably, several common variables impact the injury severity outcomes of both vehicles across both method types, among which the V1 truck and V2 passenger car have opposing effects.

Furthermore, SHAP values generated by the MLP network offer a visual analysis of the relationship between Δv and injury severity outcomes, highlighting their non-linear trends, in contrast to statistical methods that only indicate average effects. The SHAP values reveal minimal adverse effects on injury levels for two vehicles occur with a Δv of 0 to 10 mph, consistent with the pattern observed in the percentage of injury/fatality in RE crashes across Δv. Additionally, a marked variation in the trend of SHAP values is noted as the speed difference increases among following and leading vehicles. Notably, SHAP values associated with the following vehicle rise when the speed difference exceeds 15 mph, indicating a positive correlation between the severity of the impact and the speed difference. However, these values reach a peak at approximately 20 mph and then gradually decrease as the speed difference extends beyond 20 mph. Considering the findings, implementing dynamic speed control measures is recommended to mitigate the risk of RE crashes.

These developed methodologies uncover potential interactions among various contributors affecting both drivers, rather than concentrating exclusively on a single party. This heterogeneity, neglected in traditional statistical or data-driven methods with a single dependent variable, offers valuable insights for enhancing safety measures.

Based on the findings, some recommendations could be developed to reduce the injury outcomes of rear-end crashes. Stricter enforcement should be implemented for vehicles operating at improper speed compared to other vehicles. Comprehensive performance and safety checks should be conducted for vehicles aged over 10 years, with particular attention to their power and braking performance. Education programs should be developed for drivers aged 30–45 years old, as they are more prone to causing severe injury outcomes in RE crashes. Additional lighting facilities could be installed in rural areas, particularly in identified crash hotspots. Moreover, implementing variable speed limit systems could significantly reduce speed variations based on traffic flow and driving conditions.

Nevertheless, the current study has certain limitations. Future research could gain insights by examining the interactions between crash rate/severity and real-time speed/traffic characteristics in RE crashes. Moreover, the specific trajectory of the vehicle before the crash could be collected to explore the effects of braking and lane-changing maneuvers on the injury severity outcomes at aggregate levels.

7. Author Statement

The authors declare no conflict of interest. All authors reviewed the results and approved the final manuscript.

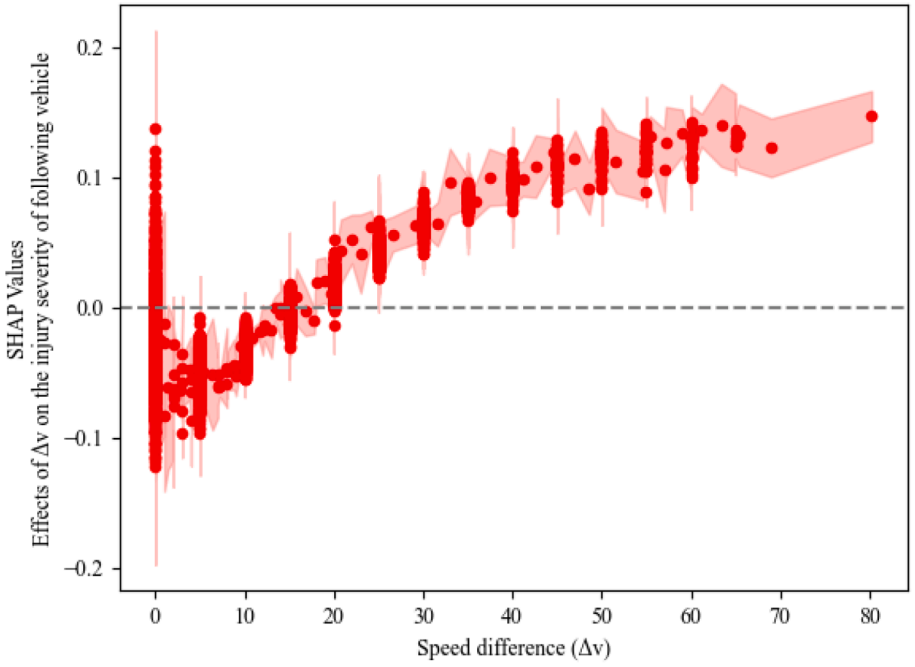

(a) Following vehicle

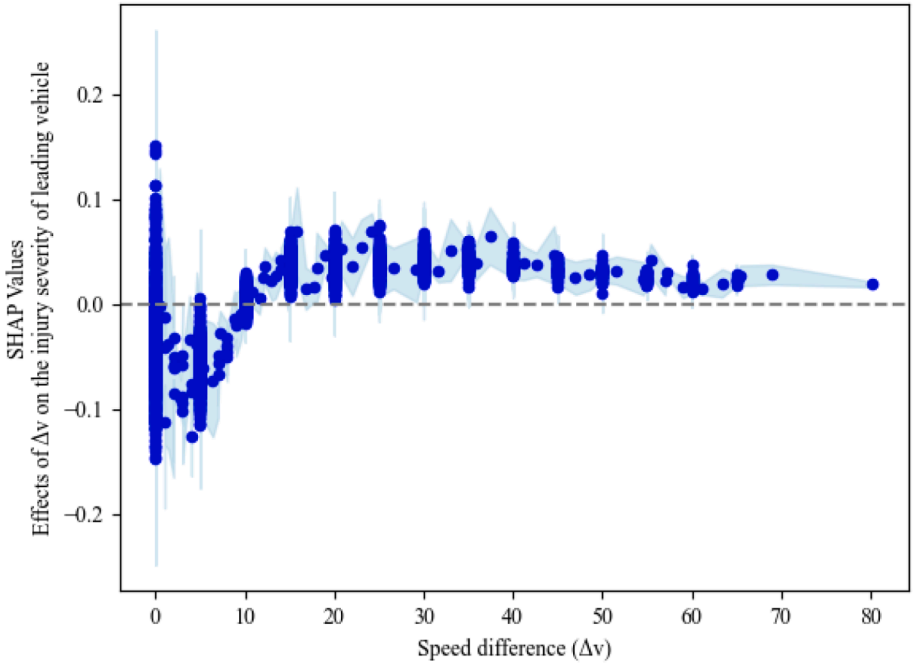

(b) Leading vehicle

Fig.10. Effects of speed difference on injury severity of following and leading vehicle measured by SHAP values.

CRediT authorship contribution statement

Chenzhu Wang: Writing – review & editing, Writing – original draft, Methodology, Data curation, Conceptualization. **Mohamed Abdel-Aty:** Writing – review & editing, Writing – original draft, Supervision, Conceptualization. **Lei Han:** Writing – review & editing, Writing – original draft, Methodology, Data curation, Conceptualization. **Said M. Easa:** Writing – review & editing, Writing – original draft, Supervision.

Declaration of competing interest

The authors declare that they have no known competing financial interests or personal relationships that could have appeared to influence the work reported in this paper.

Data availability

The authors do not have permission to share data.

Appendix A

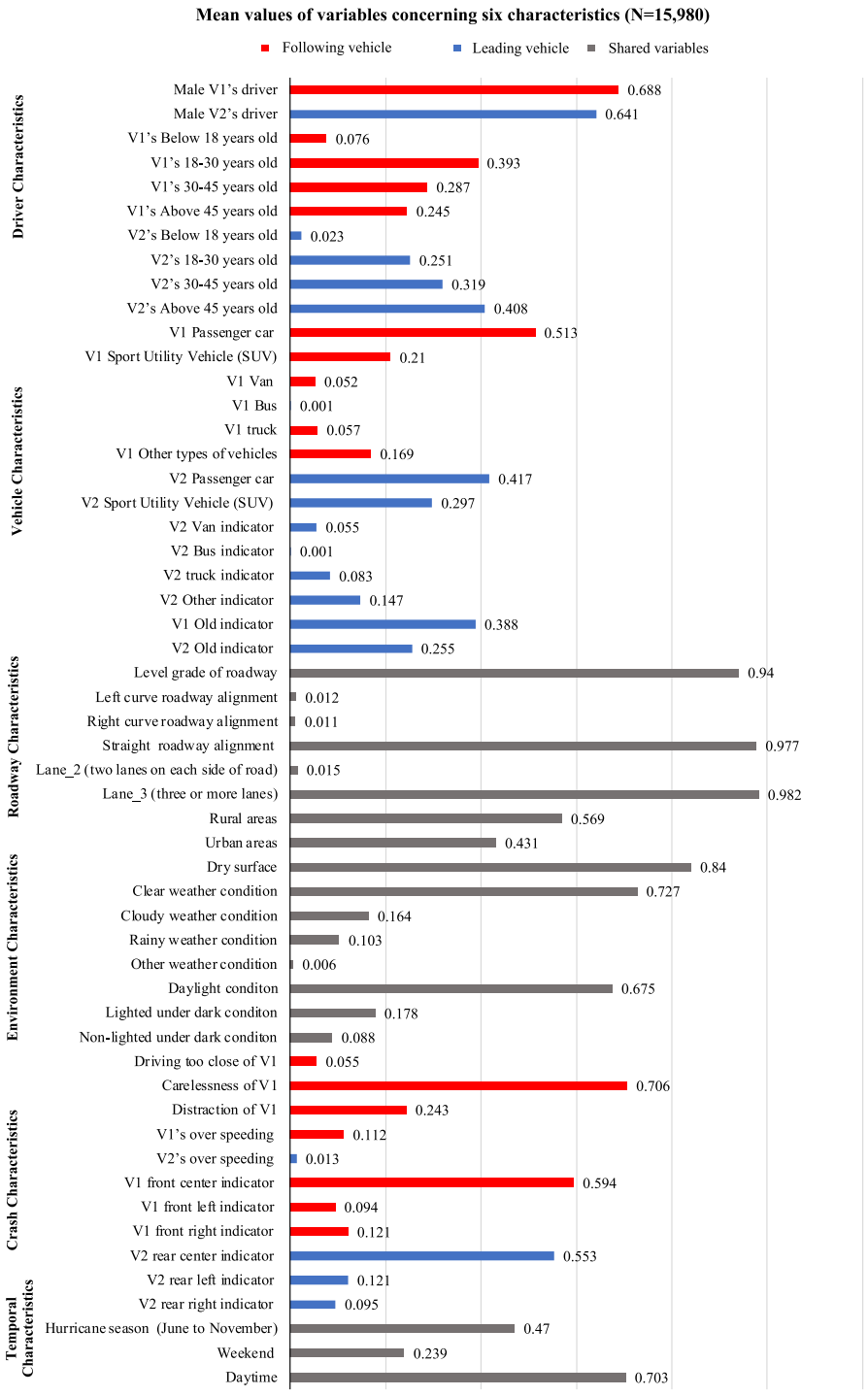

Note: The mean value of the speed difference is 14.090.

Fig. A1.

Table A1
Model results of injury severity of freeway two-vehicle rear-end crashes (t-statistics in parentheses) based on correlated joint RPBP model.

Variable	Model Estimate		Marginal effects	
	Following vehicle	Leading vehicle	Following vehicle	Leading vehicle
Constant	−0.177 (−2.34)	−1.072 (−20.09)		
Driver Characteristics				
Male V1′s driver (1 if male, 0 otherwise)	−0.285 (−7.24)		−0.0922	
Standard deviation	***0.187 (8.68)***			
Male V2′s driver (1 if male, 0 otherwise)		−0.278 (−11.38)		−0.0578
V1′s 30–45 years indicator (1 if age between 30–45 years, 0 otherwise)		0.079 (2.86)		0.0136
V2′s 30–45 years indicator (1 if age between 30–45 years, 0 otherwise)	−0.073 (−2.75)		−0.0328	
V2′s Above 45 years indicator (1 if the age of V2′s driver is above 45 years, 0 otherwise)		0.082 (3.36)		0.0171
Vehicle Characteristics				
V1 Passenger car indicator (1 if passenger car, 0 otherwise)		−0.064 (−2.58)		−0.0124
V1 truck indicator (1 if truck, 0 otherwise)	−0.562 (−7.85)	0.275 (5.27)	−0.2489	0.1913
V2 Passenger car indicator (1 if passenger car, 0 otherwise)	−0.456 (−14.30)	0.116 (4.61)	−0.2029	0.1790
V2 SUV indicator (1 if sport utility vehicle (SUV), 0 otherwise)	−0.314 (−9.58)		−0.1391	
V2 Van indicator (1 if van, 0 otherwise)	−0.269 (−4.86)		−0.1200	
Roadway Characteristics				
Level indicator (1 if the roadway's grade is level, 0 otherwise)	−0.117 (−2.18)		−0.0514	
Standard deviation	***0.136 (6.78)***			
Rural areas indicator (1 if roadway is rural, 0 otherwise)	0.053 (2.08)		0.0237	
Environmental Characteristics				
Clear indicator (1 if clear, 0 otherwise)	−0.208 (−6.31)		−0.0924	
Rainy indicator (1 if rainy, 0 otherwise)	−0.251 (−5.12)		−0.1098	
Cloudy indicator (1 if cloudy, 0 otherwise)		0.248 (7.73)		0.0517
Lighted under dark indicator (1 if the roadway is lighted during nighttime, 0 otherwise)	0.174 (3.74)	0.159 (3.53)	0.0734	0.0407
Non-lighted under dark indicator (1 if the roadway is not lighted during nighttime, 0 otherwise)	0.349 (6.50)	0.328 (6.20)	0.1511	0.0816
Crash Characteristics				
Speed difference indicator (the speed difference between the following and leading vehicle)	0.009 (11.01)	0.007 (8.53)	0.0041	0.0026
Distraction indicator (1 if crash occurred due to distraction of V1′s driver, 0 otherwise)		0.072 (2.68)		0.0151
V1′s over speeding indicator (1 if exceeding the speed limit, 0 otherwise)	0.367 (10.05)	0.356 (9.76)	0.1636	0.0878
V1 front center indicator (1 if V1′s most damage area is front center, 0 otherwise)		0.103 (4.09)		0.0219
V1 front left indicator (1 if V1′s most damage area is front left bumper, 0 otherwise)	−0.307 (−6.61)		−0.1360	
V1 front right indicator (1 if V1′s most damage area is front right bumper, 0 otherwise)	−0.323 (−7.77)		−0.1454	
V2 rear center indicator (1 if V2′s most damage area is rear center, 0 otherwise)	−0.261 (−9.77)	−0.116 (−2.63)	−0.1166	−0.0812
V2 rear right indicator (1 if V2′s most damage area is rear right bumper, 0 otherwise)		−0.109 (−2.54)		−0.0239
Temporal Characteristics				
Day indicator (1 if crash occurred during daytime, 0 otherwise)	−0.288 (−6.69)	−0.303 (−6.59)	−0.1308	−0.0810
Standard deviation		***0.136 (6.78)***		
Heterogeneity in the means of RP				
Male V1′s driver (1 if male, 0 otherwise) [V1]: V1′s 18–30 years indicator (1 if age between 18–30 years, 0 otherwise)	0.125 (2.56)			
Level indicator (1 if the roadway's grade is level, 0 otherwise) [V1]: V1′s 18–30 years indicator (1 if age between 18–30 years, 0 otherwise)	−0.115 (−2.81)			
Level indicator (1 if the roadway's grade is level, 0 otherwise) [V1]: Hurricane indicator (1 if crash occurred in hurricane season (June to November), 0 otherwise)	0.065 (2.62)			
Diagonal Elements of the Cholesky matrix (t-stats in parentheses), and correlation coefficients [in brackets] for the correlated RP				
Male V1′s driver (1 if male, 0 otherwise) [V1] | Level indicator (1 if the roadway's grade is level, 0 otherwise) [V1]	0.130 (5.42) [0.696]			
Male V1′s driver (1 if male, 0 otherwise) [V1] | Day indicator (1 if crash occurred during daytime, 0 otherwise) [V2]	−0.204 (−13.06) [0.266]			
Level indicator (1 if the roadway's grade is level, 0 otherwise) [V1] | Day indicator (1 if crash occurred during daytime, 0 otherwise) [V2]	0.370 (22.89) [0.854]			
ρ	0.612 (46.89)			
Number of parameters (K)	46			
Number of observations (N)	15,890			
Log-likelihood at zero	−17733.240			
Log-likelihood at convergence	−12404.043			
$\rho^2 = 1 - LL(\beta)/LL(0)$	0.301			
Corrected ρ^2	0.298			
Corrected AIC	24900.359			

Note: V1 and V2 denotes the following vehicle and leading vehicle, respectively. And "Male V1's driver (1 if male, 0 otherwise) [V1]" means that this variable is identified as a random parameter specific to V1 (following vehicle).

References

Abdel-Aty, M., Abdelwahab, H., 2004. Modeling Rear-End Collisions Including the Role of Drivers Visibility and Light Truck Vehicles Using a Nested Logit Structure. Accid. Anal. Prev. 36 (3), 47–456.

Abdulnabi, A.H., Wang, G., Lu, J., Jia, K., 2015. Multi-task CNN model for attribute prediction. IEEE Trans. Multimedia 17 (11), 1949–1959.

Ahmadi, A., Jahangiri, A., Berardi, V., Machiani, S., 2020. Crash severity analysis of rear-end crashes in California using statistical and machine learning classification methods. Journal of Transportation Safety and Security 12 (4), 522–546.

Ahmed, S., Cohen, J., Anastasopoulos, P., 2021. A correlated random parameters with heterogeneity in means approach of deer-vehicle collisions and resulting injury-severities. Analytic Methods in Accident Research 30, 100160.

Anderson, R., Baldock, M., 2008. Vehicle improvements to reduce the number and severity of rear end crashes. Centre for Automotive Safety Research. Centre for Automotive Safety Research (CASR).

Behnood, A., Al-Bdairi, N., 2020. Determinant of injury severities in large truck crashes: A weekly instability analysis. Saf. Sci. 131, 104911.

Beljaards, L., Elmahdy, M., Verbeek, F., Staring, M., 2020. A Cross-Stitch Architecture for Joint Registration and Segmentation in Adaptive Radiotherapy. Proceedings of Machine Learning Research 121, 62–73.

Bhat, C., 2018. New matrix-based methods for the analytic evaluation of the multivariate cumulative normal distribution function. Transp. Res. B 109, 238–256.

Brach, M., Mason, J., Brach, R., 2022. Vehicle Accident Analysis and Reconstruction Methods. Publisher Solutions, LCC Albany, NY, Sherry Dickinson Nigam.

Chatterjee, I., 2016. Understanding driver contributions to rear-end crashes on congested freeways and their implications for future safety measures. University of Minnesota. Doctoral dissertation.

Chen, C., Zhang, G., Tarefder, R., Ma, J., Wei, H., Guan, H., 2015. A multinomial logit model-Bayesian network hybrid approach for driver injury severity analyses in rear-end crashes. Accid. Anal. Prev. 80, 76–88.

Chen, C., Zhang, G., Yang, J., Milton, J., Alcantara, A., 2016. An explanatory analysis of driver injury severity in rear-end crashes using a decision table/Naive Bayes (DTNB) hybrid classifier. Accid. Anal. Prev. 90, 95–107.

Christofides, L., Stengos, T., Swidinsky, R., 1997. On the calculation of marginal effects in the bivariate probit model. Econ. Lett. 54 (3), 203–208.

Das, A., Abdel-Aty, M., 2011. A combined frequency–severity approach for the analysis of rear-end crashes on urban arterials. Saf. Sci. 49, 1156–1163.

Das, S., Brimley, B., Lindheimer, T., Zupancich, M., 2018. Association of reduced visibility with crash outcomes. IATSS Research 42 (3), 143–151.

Doecke, S., Dutschke, J., Baldock, M., Kloeden, C., 2021. Travel speed and the risk of serious injury in vehicle crashes. Accid. Anal. Prev. 161, 106359.

Egger, J., Pepe, A., Gsaxner, C., Jin, Y., Li, J., Kern, R., 2021. Deep learning—a first meta-survey of selected reviews across scientific disciplines, their commonalities, challenges and research impact. Peer J Computer Science 7, e773.

Elvik, R., 2013. A re-parameterisation of the Power Model of the relationship between the speed of traffic and the number of accidents and accident victims. Accid. Anal. Prev. 50, 854–860.

Elvik, R., Vadeby, A., Hels, T., Van Schagen, I., 2019. Updated estimates of the relationship between speed and road safety at the aggregate and individual levels. Accid. Anal. Prev. 123, 114–122.

Fountas, G., Anastasopoulos, P., Abdel-aty, M., 2018. Analysis of accident injury-severities using a correlated random parameters ordered probit approach with time variant covariates. Analytic Methods in Accident Research 18, 57–68.

Fountas, G., Fonzone, A., Olowosegun, A., McTigue, C., 2021. Addressing unobserved heterogeneity in the analysis of bicycle crash injuries in Scotland: a correlated random parameters ordered probit approach with heterogeneity in means. Analytic Methods in Accident Research 32, 100181.

Greene, W., 2012. Econometric Analysis, 7th Edition. Prentice Hall, Englewood Cliffs.

Han, L., Yu, R., Wang, C., Abdel-Aty, M., 2024. Transformer-based modeling of abnormal driving events for freeway crash risk evaluation. Transportation Research Part C: Emerging Technologies 165, 104727.

Harb, R., Radwan, E., Yan, X., Abdel-Aty, M., 2007. Light Truck Vehicles (LTVs) Contribution to Rear End Collisions. Accid. Anal. Prev. 39 (5), 1026–1036.

Hauer, E., 1971. Accidents, overtaking and speed control. Accid. Anal. Prev. 3, 1–13.

Hauer, E., 2009. Speed and Safety. Transp. Res. Rec. 2103, 10–17.

Knill, G., Fawcett, G., 1981. Applications: Skid Marks Estimate Speed. The Mathematics Teacher 74 (9), 722–724.

Kokkinos, I., 2017. Ubernet: Training a universal convolutional neural network for low-, mid-, and high-level vision using diverse datasets and limited memory. In: In Proceedings of the IEEE Conference on Computer Vision and Pattern Recognition, pp. 6129–6138.

Li, Y., Wu, D., Chen, Q., Lee, J., Long, K., 2021. Exploring transition durations of rear-end collisions based on vehicle trajectory data: A survival modeling approach. Accid. Anal. Prev. 159, 106271.

Liu, Q., Wang, D., Jia, Y., Luo, S., Wang, C., 2022. A multi-task based deep learning approach for intrusion detection. Knowl.-Based Syst. 238, 107852.

Long, M., Cao, Z., Wang, J., Yu, P., 2017. Learning multiple tasks with multilinear relationship networks. Adv. Neural Inf. Proces. Syst. 30.

Lundberg, S., Lee, S., 2017. A unified approach to interpreting model predictions. Adv. Neural Inf. Proces. Syst. 30.

Luo, P., Zhang, X., Meng, R., 2023. Co-attention learning cross time and frequency domains for fault diagnosis. Cognitive Robotics 3, 34–44.

Ma, W., Miao, Y., He, Z., Wang, L., Abdel-Aty, 2024. Expressway Rear-End Conflict Pattern Classification and Modeling. Transp. Res. Rec. 2678 (1), 612–628.

Mannering, F., 2018. Temporal instability and the analysis of highway accident data. Analytic Methods in Accident Research 17, 1–13.

Mannering, F., Shankar, V., Bhat, C., 2016. Unobserved heterogeneity and the statistical analysis of highway accident data. Analytic Methods in Accident Research 11, 1–16.

Mannering, F., Bhat, C., Shankar, V., Abdel-Aty, M., 2020. Big data, traditional data and the tradeoffs between prediction and causality in highway-safety analysis. Analytic Methods in Accident Analysis 25, 100113.

McFadden, D., Train, K., 2000. Mixed MNL models for discrete response. J. Appl. Economet. 15, 447–470.

Milton, J., Shankar, V., Mannering, F., 2008. Highway accident severities and the mixed logit model: an exploratory empirical analysis. Accid. Anal. Prev. 40 (1), 260–266.

Misra, I., Shrivastava, A., Gupta, A., Hebert, M., 2016. Cross-stitch networks for multi-task learning. In Proceedings of the IEEE conference on computer vision and pattern recognition, 3994-4003.

Moussa, G., Owais, M., Dabbour, E., 2022. Variance-based global sensitivity analysis for rear-end crash investigation using deep learning. Accid. Anal. Prev. 165, 106514.

National Highway Traffic Safety Administration (NHTSA), 2020. Traffic safety facts: A Compilation of Motor Vehicle Crash Data. National Highway Traffic Safety Administration, Washington DC, p. 20590.

Nieve, J., Formica, C., Ruffing, J., Zion, M., Garrett, P., Lindsay, R., Cosman, F., 2009. Males have larger skeletal size and bone mass than females, despite comparable body size. J. Bone Miner. Res. 20 (3), 365–550.

Nweke, H., The, Y., Al-garadi, M., Alo, U., 2018. Deep learning algorithms for human activity recognition using mobile and wearable sensor networks: State of the art and research challenges. Expert Syst. Appl. 105 (1), 233–261.

Owais, M., Alshehri, A., Gyani, J., Aljarbou, M., Alsulamy, S., 2024. Prioritizing rear-end crash explanatory factors for injury severity level using deep learning and global sensitivity analysis. Expert Syst. Appl. 245, 123114.

Paka, W.S., Bansal, R., Kaushik, A., Sengupta, S., Chakraborty, T., 2021. Cross-SEAN: A cross-stitch semi-supervised neural attention model for COVID-19 fake news detection. Applied Soft Computing 107, 107393.

Pande, A., Abdel-Aty, M., 2006. Comprehensive Analysis of the Relationship Between Real-Time Traffic Surveillance Data and Rear-End Crashes on Freeways. Transportation Research Record: Journal of the Transportation Research Board. 1953 (1), 31–40.

Pande, A., Abdel-Aty, M., 2008. A Computing Approach Using Probabilistic Neural Networks for Instantaneous Appraisal of Rear-End Crash Risk. Comput. Aided Civ. Inf. Eng. 23 (7), 549–559.

Qi, Y., Srinivasan, R., Teng, H., Baker, R., 2013. Analysis of the frequency and severity of rear-end crashes in work zones. Traffic Inj. Prev. 14, 61–72.

Rana, T.A., Sikder, S., Pinjari, A.R., 2010. Copula-based method for addressing endogeneity in models of severity of traffic crash injuries: Application to two-vehicle crashes. Transp. Res. Rec. 2147 (1), 75–87.

Ribeiro, M., Singh, S., Guestrin, C., 2016. "Why should I trust you?" Explaining the predictions of any classifier. In Proceedings of the 22nd ACM SIGKDD international conference on knowledge discovery and data mining, 1135–1144.

Richard, P., 2021. The Facts About Rear-End Accidents. The National Law Review 11, 180. https://www.natlawreview.com/article/facts-about-rear-end accidents.

Santos, K., Dias, J., Amado, C., 2022. A literature review of machine learning algorithms for crash injury severity prediction. J. Saf. Res. 80, 254–269.

Schulz, M., Yeo, B., Vogelstein, J., Mourao-Miranada, J., Kather, J., Kording, K., Kording, J., Richards, B., Bzdok, D., 2020. Different scaling of linear models and deep learning in UKBiobank brain images versus machine-learning datasets. Nat. Commun. 11, 4238.

Solomon, D., 1964. Accidents on Main Rural Highways Related to Speed, Driver, and Vehicle. U.S, DOT/ FHWA https://safety.fhwa.dot.gov/speedmgt/ref_mats/fhwasa1304/2_40.htm.

Song, D., Yang, X., Yang, Y., Cui, P., Zhu, G., 2023. Bivariate Joint Analysis of Injury Severity of Drivers in Truck-Car Crashes Accommodating Multilayer Unobserved Heterogeneity. 190, 107175.

Soole, D., Watson, B., Fleiter, J., 2013. Effects of average speed enforcement on speed compliance and crashes: A review of the literature. Accid. Anal. Prev. 54, 46–56.

Štrumbelj, E., Kononenko, I., 2014. Explaining prediction models and individual predictions with feature contributions. Knowl. Inf. Syst. 41, 647–665.

Stylianou, K., Dimitriou, L., 2018. Analysis of Rear-End Conflicts in Urban Networks using Bayesian Networks. Transportation Research Record: Journal of the Transportation Research Board 2762 (38), 302–312.

Tan, M., Hu, C., Chen, J., Wang, L., Li, Z., 2022. Multi-node load forecasting based on multi-task learning with modal feature extraction. Eng. Appl. Artif. Intel. 112, 104856.

Vandenhende, S., Georgoulis, S., Van Gansbeke, W., Proesmans, M., Dai, D., Van Gool, L., 2021. Multi-task learning for dense prediction tasks: A survey. IEEE Trans. Pattern Anal. Mach. Intell. 44 (7), 3614–3633.

Wang, X., Abdel-Aty, M., 2006. Temporal and spatial analyses of rear-end crashes at signalized intersections. Accid. Anal. Prev. 38, 1137–1150.

Wang, C., Chen, F., Cheng, J., Easa, S.M., 2024. Modeling injury severities of single and multi-vehicle freeway crashes considering spatiotemporal instability and unobserved heterogeneity. Transportation letters 16 (3), 234–262.

Wang, C., Chen, F., Zhang, Y., Wang, S., Yu, B., Cheng, J., 2022a. Temporal stability of factors affecting injury severity in rear-end and non-rear-end crashes: A random parameter approach with heterogeneity in means and variances. Analytic Methods in Accident Research 35, 100219.

Wang, C., Abdel-Aty, M., Han, L., 2024a. Effects of speed difference on injury severity of freeway rear-end crashes: Insights from correlated joint random parameters bivariate probit models and temporal instability. Analytic Methods in Accident Research 42, 100320.

Wang, Z., Huang, H., Tang, J., Hu, L., 2024b. A deep reinforcement learning-based approach for autonomous lane-changing velocity control in mixed flow of vehicle group level. Expert Syst. Appl. 238, 122158.
Wang, L., Zou, L., Abdel-Aty, M., Ma, W., 2022b. Expressway Rear-End Crash Evolution Analysis under Different Traffic States. Transport Dynamics (TTRB), Aug, Transportmetrica B, p. 2022.
Washington, S., Karlaftis, M., Mannering, F., Anastasopoulos, P., 2020. Statistical and Econometric Methods for Transportation Data Analysis, 3rd edition. CRC Press, Taylor and Francis Group, New York, NY.
Wu, Y., Abdel-Aty, M., Wang, L., Rahman, S., 2020. Combined connected vehicles and variable speed limit strategies to reduce rear-end crash risk under fog conditions. J. Intell. Transp. Syst. Technol. Plann. Oper. 24 (5), 1–20.
Zeng, Q., Gu, W., Zhang, X., Wen, H., Lee, J., Hao, W., 2019. Analyzing freeway crash severity using a bayesian spatial generalized ordered logit model with conditional autoregressive priors. Accid. Anal. Prev. 127, 87–95.
Zhang, K., Hassan, M., 2019. Identifying the Factors Contributing to Injury Severity in Work Zone Rear-End Crashes. Journal of advanced transportation 2019 (1), 4126102.
Zhang, J., Ma, C., Chen, P., Li, M., Wang, R., Gao, Z., 2023. Co-Attention based Cross-Stitch Network for Parameter Prediction of Two-Phase Flow. IEEE Trans. Instrum. Meas. 72, 2516212.
Zou, R., Yang, H., Yu, W., Yu, H., Chen, C., Zhang, G., Ma, D., 2023. Analyzing driver injury severity in two-vehicle rear-end crashes considering leading-following configurations based on passenger car and light truck involvement. Accid. Anal. Prev. 193, 107298.